Unpolarised SIDIS studies at COMPASS

Jan Matoušek
Charles University, Prague, Czechia
on behalf of the COMPASS collaboration

18. 11. 2020
International Workshop on Hadron Structure and Spectroscopy

IWHSS 2020

CHARLES UNIVERSITY
Faculty of mathematics
and physics

COMPASS

Outline

Introduction: COMPASS

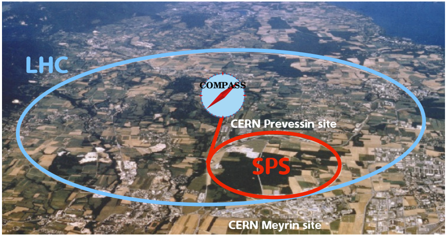

It is located at M2 beamline of CERN's SPS.

- Collaboration: 24 institutes, 13 countries.
- Fixed target, multi-purpose.
- Broad research programme:
  - SIDIS: μ^+ beam and L/T-polarised proton (NH_3) or deuteron (^6LiD) target (beam 160 GeV/c, 200 GeV/c in 2011)
  - Hadron spectroscopy: hadron beams and nuclear targets.
  - Drell–Yan: 190 GeV/c π^- beam and $p^\uparrow$, Al and W targets.
  - DVCS and SIDIS: 160 GeV/c $\mu^\pm$ beam and liquid H_2 target.

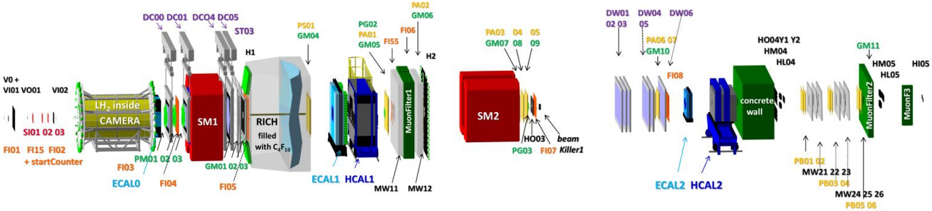

2016–2017 setup with CAMERA recoil proton detector and ECAL0 calorimeter for DVCS studies.

The cross section for producing a hadron h in DIS on unpolarised target $\ell \mathrm{N} \to \ell' \mathrm{hX}$:
[A. Bacchetta *et al.*, JHEP 0702 (2007)]

$$\frac{\mathrm{d}\sigma}{\mathrm{d}x\mathrm{d}y\mathrm{d}z\mathrm{d}\phi_\mathrm{h}\mathrm{d}P_\mathrm{T}^2} = \frac{2\pi\alpha^2}{xyQ^2}\frac{y^2}{2(1-\varepsilon)}\left(1+\frac{2xM^2}{Q^2}\right)\Big(F_{\mathrm{UU,T}} + \varepsilon F_{\mathrm{UU,L}}$$
$$+ \sqrt{2\varepsilon(1+\varepsilon)}F_{\mathrm{UU}}^{\cos\phi_\mathrm{h}}\cos\phi_\mathrm{h} + \varepsilon F_{\mathrm{UU}}^{\cos 2\phi_\mathrm{h}}\cos 2\phi_\mathrm{h} + \lambda\sqrt{2\varepsilon(1-\varepsilon)}F_{\mathrm{LU}}^{\sin\phi_\mathrm{h}}\sin\phi_\mathrm{h}\Big)$$
$$= \sigma_0\left(1 + \varepsilon_1 A_{\mathrm{UU}}^{\cos\phi_\mathrm{h}}\cos\phi_\mathrm{h} + \varepsilon_2 A_{\mathrm{UU}}^{\cos 2\phi_\mathrm{h}}\cos 2\phi_\mathrm{h} + \lambda\varepsilon_3 A_{\mathrm{LU}}^{\sin\phi_\mathrm{h}}\sin\phi_\mathrm{h}\right)$$

- where x, y, Q^2 are usual DIS variables,
- λ is the beam polarisation (≈ 0.8 at COMPASS),
- $\varepsilon \approx \frac{1-y}{1-y+\frac{1}{2}y^2}$, M nucleon mass,
- z is the fraction of γ^* energy carried by h.
- P_T is the transverse momentum of h in the γN frame, ϕ_h is its azimuthal angle.
- $F_{\mathrm{XU}}^{f(\phi_\mathrm{h})}(x, z, P_\mathrm{T}^2, Q^2)$ are structure functions.
- $A_{\mathrm{XU}}^{f(\phi_\mathrm{h})}(x, z, P_\mathrm{T}^2, Q^2)$ are commonly called azimuthal asymmetries.

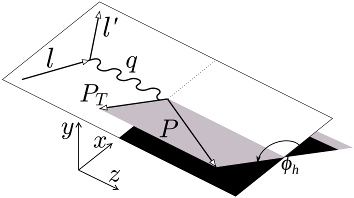

SIDIS in the γ–nucleon frame.

The cross section for producing a hadron h in DIS on unpolarised target $\ell \mathrm{N} \to \ell' \mathrm{hX}$:
[A. Bacchetta *et al.*, JHEP 0702 (2007)]

$$\frac{\mathrm{d}\sigma}{\mathrm{d}x\mathrm{d}y\mathrm{d}z\mathrm{d}\phi_\mathrm{h}\mathrm{d}P_\mathrm{T}^2} = \frac{2\pi\alpha^2}{xyQ^2}\frac{y^2}{2(1-\varepsilon)}\left(1+\frac{2xM^2}{Q^2}\right)\left(F_{\mathrm{UU,T}} + \varepsilon F_{\mathrm{UU,L}}\right.$$
$$\left. + \sqrt{2\varepsilon(1+\varepsilon)}F_{\mathrm{UU}}^{\cos\phi_\mathrm{h}}\cos\phi_\mathrm{h} + \varepsilon F_{\mathrm{UU}}^{\cos 2\phi_\mathrm{h}}\cos 2\phi_\mathrm{h} + \lambda\sqrt{2\varepsilon(1-\varepsilon)}F_{\mathrm{LU}}^{\sin\phi_\mathrm{h}}\sin\phi_\mathrm{h}\right)$$
$$= \sigma_0\left(1 + \varepsilon_1 A_{\mathrm{UU}}^{\cos\phi_\mathrm{h}}\cos\phi_\mathrm{h} + \varepsilon_2 A_{\mathrm{UU}}^{\cos 2\phi_\mathrm{h}}\cos 2\phi_\mathrm{h} + \lambda\varepsilon_3 A_{\mathrm{LU}}^{\sin\phi_\mathrm{h}}\sin\phi_\mathrm{h}\right)$$

- where x, y, Q^2 are usual DIS variables,
- λ is the beam polarisation (≈ 0.8 at COMPASS),
- $\varepsilon \approx \frac{1-y}{1-y+\frac{1}{2}y^2}$, M nucleon mass,
- z is the fraction of γ^* energy carried by h.
- P_T is the transverse momentum of h in the γN frame, ϕ_h is its azimuthal angle.
- $F_{\mathrm{XU}}^{f(\phi_\mathrm{h})}(x, z, P_\mathrm{T}^2, Q^2)$ are structure functions.
- $A_{\mathrm{XU}}^{f(\phi_\mathrm{h})}(x, z, P_\mathrm{T}^2, Q^2)$ are commonly called azimuthal asymmetries.

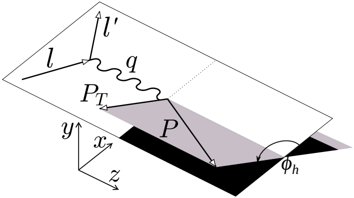

SIDIS in the γ–nucleon frame.

Introduction: Unpolarised SIDIS cross section

The structure functions in terms of TMD PDFs and TMD FFs, up to order $1/Q$:

$$F_{\mathrm{UU,T}} = \mathcal{C}\left[f_1 D_1\right],$$

$$F_{\mathrm{UU,L}} = 0,$$

Cahn effect

$$F_{\mathrm{UU}}^{\cos\phi_{\mathrm{h}}} = \frac{2M}{Q}\mathcal{C}\left[-\overbrace{\frac{\hat{\boldsymbol{h}}\cdot\boldsymbol{k}_{\mathbf{T}}}{M} f_1 D_1}^{\text{Cahn effect}} - \frac{(\hat{\boldsymbol{h}}\cdot\boldsymbol{p}_\perp)k_{\mathrm{T}}^2}{M^2 M_{\mathrm{h}}} h_1^\perp H_1^\perp + \ldots\right]$$

$$F_{\mathrm{UU}}^{\cos 2\phi_{\mathrm{h}}} = \mathcal{C}\left[-\frac{2(\hat{\boldsymbol{h}}\cdot\boldsymbol{k}_{\mathbf{T}})(\hat{\boldsymbol{h}}\cdot\boldsymbol{p}_\perp) - \boldsymbol{k}_{\mathbf{T}}\cdot\boldsymbol{p}_\perp}{M M_{\mathrm{h}}} h_1^\perp H_1^\perp\right]$$

$$F_{\mathrm{UU}}^{\sin\phi_{\mathrm{h}}} = \frac{2M}{Q}\mathcal{C}\left[\ldots\right]$$

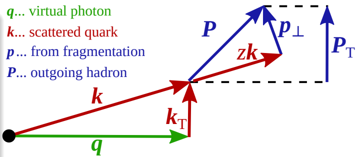

Momentum vectors
$\boldsymbol{P}_{\mathbf{T}} = z\boldsymbol{k}_{\mathbf{T}} + \boldsymbol{p}_\perp$

- $f_1(x, k_{\mathrm{T}}^2, Q^2)$ unpolarised TMD PDF,
- $h_1^\perp(x, k_{\mathrm{T}}^2, Q^2)$ Boer–Mulders function,
- $D_1(z, p_\perp^2, Q^2)$ unpolarised TMD FF,
- $H_1^\perp(z, p_\perp^2, Q^2)$ Collins function.
- $\hat{\boldsymbol{h}} = \boldsymbol{P}_{\mathbf{T}}/P_{\mathrm{T}}$,
- $\mathcal{C}$ = sum over flavours and convolution over $\boldsymbol{p}_\perp, \boldsymbol{k}_{\mathbf{T}}$,
- … = twist-three terms.

Observables sensitive to k_{T} and $p_\perp$:

- azimuthal asymmetries $A_{\mathrm{UU}}^{\cos\phi_{\mathrm{h}}}$, $A_{\mathrm{UU}}^{\cos 2\phi_{\mathrm{h}}}$, $A_{\mathrm{UU}}^{\sin\phi_{\mathrm{h}}}$,
  - k_{T} via Cahn effect,
  - Boer–Mulders function.
- P_{T}-dependent distributions $\propto F_{\mathrm{UU,T}} = \mathcal{C}[f_1 D_1]$.

Introduction: Unpolarised SIDIS cross section

The structure functions in terms of TMD PDFs and TMD FFs, up to order $1/Q$:

$$F_{UU,T} = \mathcal{C}\left[f_1 D_1\right],$$

$$F_{UU,L} = 0,$$

$$F_{UU}^{\cos\phi_h} = \frac{2M}{Q}\mathcal{C}\left[-\overbrace{\frac{\hat{\boldsymbol{h}}\cdot\boldsymbol{k}_T}{M} f_1 D_1}^{\text{Cahn effect}} - \frac{(\hat{\boldsymbol{h}}\cdot\boldsymbol{p}_\perp)k_T^2}{M^2 M_h} h_1^\perp H_1^\perp + \ldots\right]$$

$$F_{UU}^{\cos 2\phi_h} = \mathcal{C}\left[-\frac{2(\hat{\boldsymbol{h}}\cdot\boldsymbol{k}_T)(\hat{\boldsymbol{h}}\cdot\boldsymbol{p}_\perp) - \boldsymbol{k}_T\cdot\boldsymbol{p}_\perp}{M M_h} h_1^\perp H_1^\perp\right]$$

$$F_{UU}^{\sin\phi_h} = \frac{2M}{Q}\mathcal{C}\left[\ldots\right]$$

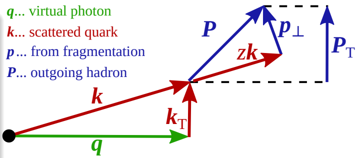

Momentum vectors
$\boldsymbol{P}_T = z\boldsymbol{k}_T + \boldsymbol{p}_\perp$

- $f_1(x, k_T^2, Q^2)$ unpolarised TMD PDF,
- $h_1^\perp(x, k_T^2, Q^2)$ Boer–Mulders function,
- $D_1(z, p_\perp^2, Q^2)$ unpolarised TMD FF,
- $H_1^\perp(z, p_\perp^2, Q^2)$ Collins function.
- $\hat{\boldsymbol{h}} = \boldsymbol{P}_T / P_T$,
- $\mathcal{C}$ = sum over flavours and convolution over $\boldsymbol{p}_\perp, \boldsymbol{k}_T$,
- … = twist-three terms.

Observables sensitive to k_T and $p_\perp$:

- azimuthal asymmetries $A_{UU}^{\cos\phi_h}$, $A_{UU}^{\cos 2\phi_h}$, $A_{UU}^{\sin\phi_h}$,
  - k_T via Cahn effect,
  - Boer–Mulders function.
- P_T-dependent distributions $\propto F_{UU,T} = \mathcal{C}[f_1 D_1]$.

Introduction: COMPASS measurements of unpolarised SIDIS

Published unpolarised SIDIS results:

- Azimuthal asymmetries on ^{6}LiD target [COMPASS, Nucl.Phys.B 886 (2014)].
- P_T-dependent multiplicities on ^{6}LiD target [COMPASS, Phys.Rev.D97 (2018)]
- Background to the asymmetries from decays of exclusive vector mesons [COMPASS, Nucl.Phys.B 956 (2020)].

Ongoing analysis presented in this talk:

- 2016–2017 data taken with 2.5 m long LH_2 target.
- Primary goal: DVCS measurement, but useful for SIDIS as well.
- Advantages:
  - pure proton target,
  - alternating $\mu^{\pm}$ beam with balanced statistics (stability tests for systematics),
  - MC development in synergy with DVCS analysis.
- Part of the data (about 11 %) used for preliminary results, released in August 2020.

Future:

- 2021 run with ^{6}LiD target (transversely polarised).

Published unpolarised SIDIS results:

- Azimuthal asymmetries on ^{6}LiD target [COMPASS, Nucl.Phys.B 886 (2014)].
- P_T-dependent multiplicities on ^{6}LiD target [COMPASS, Phys.Rev.D97 (2018)]
- Background to the asymmetries from decays of exclusive vector mesons [COMPASS, Nucl.Phys.B 956 (2020)].

Ongoing analysis presented in this talk:

- 2016–2017 data taken with 2.5 m long LH_2 target.
- Primary goal: DVCS measurement, but useful for SIDIS as well.
- Advantages:
  - pure proton target,
  - alternating $\mu^\pm$ beam with balanced statistics (stability tests for systematics),
  - MC development in synergy with DVCS analysis.
- Part of the data (about 11 %) used for preliminary results, released in August 2020.

Future:

- 2021 run with ^{6}LiD target (transversely polarised).

Published unpolarised SIDIS results:

- Azimuthal asymmetries on ^{6}LiD target [COMPASS, Nucl.Phys.B 886 (2014)].
- P_T-dependent multiplicities on ^{6}LiD target [COMPASS, Phys.Rev.D97 (2018)]
- Background to the asymmetries from decays of exclusive vector mesons [COMPASS, Nucl.Phys.B 956 (2020)].

Ongoing analysis presented in this talk:

- 2016–2017 data taken with 2.5 m long LH_2 target.
- Primary goal: DVCS measurement, but useful for SIDIS as well.
- Advantages:
  - pure proton target,
  - alternating $\mu^\pm$ beam with balanced statistics (stability tests for systematics),
  - MC development in synergy with DVCS analysis.
- Part of the data (about 11 %) used for preliminary results, released in August 2020.

Future:

- 2021 run with ^{6}LiD target (transversely polarised).

Outline

- [COMPASS, Nucl.Phys.B 886 (2014)]
- Isoscalar target, effectively deuteron.
- Unidentified charged hadrons studied.
- 1D analysis
  (bins in x, z and P_T separately).
- 3D analysis (3D grid of bins).
- Strong kinematic dependence of the $\cos\phi_h$ and $\cos 2\phi_h$ asymmetries.
- At the time, some features were not understood (e.g. positive $A_{UU}^{\cos\phi_h}$)
- Exclusive vector meson contribution has been proved important later.

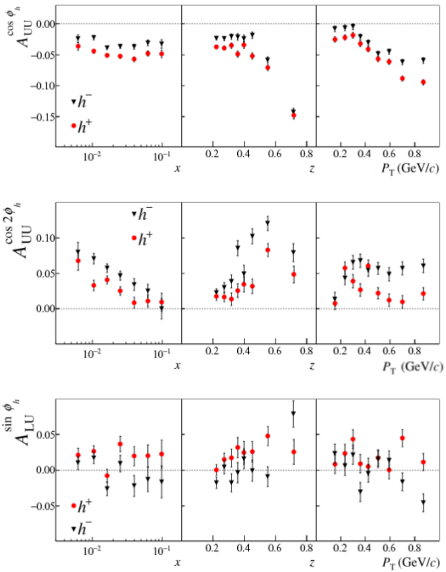

Published measurements on ^{6}LiD: Azimuthal asymmetries

- [COMPASS, Nucl.Phys.B 886 (2014)]
- Isoscalar target, effectively deuteron.
- Unidentified charged hadrons studied.
- 1D analysis
  (bins in x, z and P_T separately).
- 3D analysis (3D grid of bins).
- Strong kinematic dependence of the $\cos\phi_h$ and $\cos 2\phi_h$ asymmetries.
- At the time, some features were not understood (e.g. positive $A_{\mathrm{UU}}^{\cos\phi_\mathrm{h}}$)
- Exclusive vector meson contribution has been proved important later.

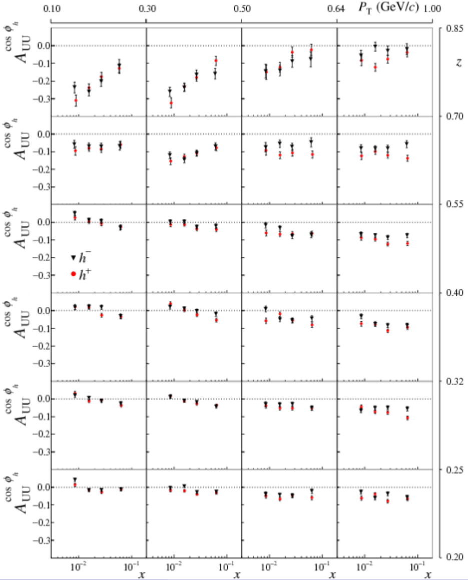

Published measurements on ^{6}LiD: P_{T}-dependent multiplicities

- [COMPASS, Phys.Rev.D97 (2018)]
- 4D analysis
  (bins in x, Q^2, z and P_{T}^2)
- Unidentified charged hadrons studied.
- QED radiative effects taken into account.
- Contribution of the decay of exclusive vector mesons
  - Contamination estimated from HEPGEN MC generator [A. Sandacz & P. Sznajder, arXiv:1207.0333].
  - Subtracted in each bin.
  - ρ^0: small P_{T}, large z, small Q^2.
  - ϕ: tiny P_{T}, medium z, small Q^2.

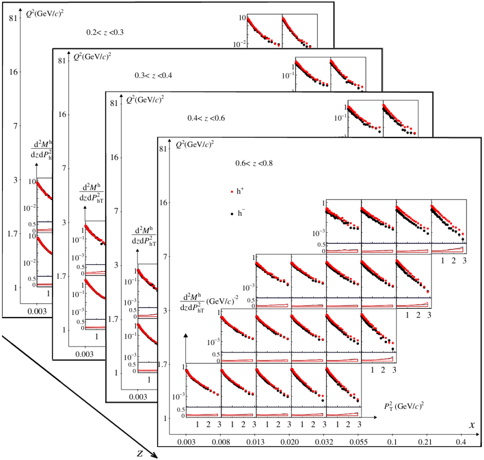

- [COMPASS, Phys.Rev.D97 (2018)]
- 4D analysis
  (bins in x, Q^2, z and P_T^2)
- Unidentified charged hadrons studied.
- QED radiative effects taken into account.
- Contribution of the decay of exclusive vector mesons
  - Contamination estimated from HEPGEN MC generator [A. Sandacz & P. Sznajder, arXiv:1207.0333].
  - Subtracted in each bin.
  - ρ^0: small P_T, large z, small Q^2.
  - ϕ: tiny P_T, medium z, small Q^2.

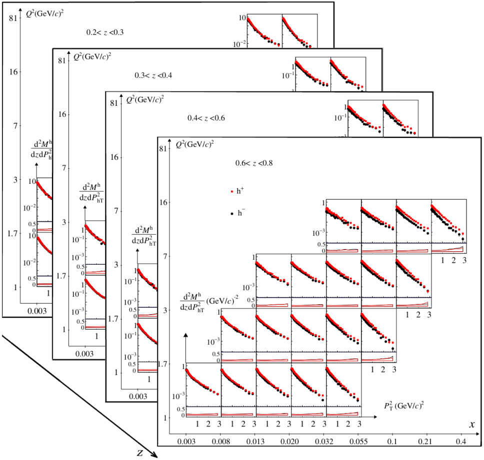

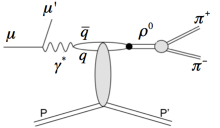

Diffractively produced $\rho^0 \to \pi^+\pi^-$, creating a background to SIDIS.

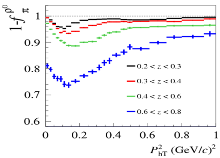

$1 - \rho^0$ contamination fraction.

- [COMPASS, Nucl.Phys.B 956 (2020)].
- The exclusive VMs inherit γ^* polarisation.
- The decay hadrons obtain large azimuthal modulations. Especially in $\cos\phi_\mathrm{h}$.
- They were measured in the data selecting
  - only $\mu' h^+ h^-$,
  - $z_1 + z_2 > 0.95$.
- The contamination fraction from HEPGEN.
- Subtraction at the asymmetry level.

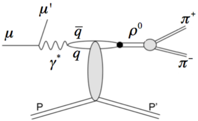

Diffractive ρ^0 production.

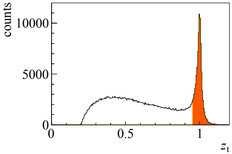

Total z for h^+h^-.

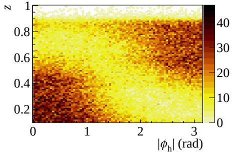

ϕ_h–z correlation.

- [COMPASS, Nucl.Phys.B 956 (2020)].
- The exclusive VMs inherit γ^* polarisation.
- The decay hadrons obtain large azimuthal modulations. Especially in $\cos\phi_{\mathrm{h}}$.
- They were measured in the data selecting
  - only $\mu' \mathrm{h}^+ \mathrm{h}^-$,
  - $z_1 + z_2 > 0.95$.
- The contamination fraction from HEPGEN.
- Subtraction at the asymmetry level.

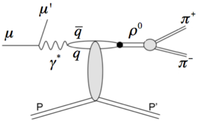

Diffractive ρ^0 production.

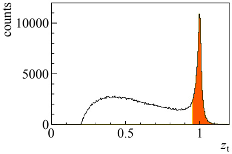

Total z for $\mathrm{h}^+\mathrm{h}^-$.

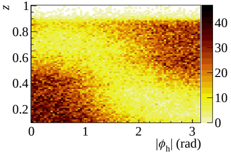

ϕ_{h}–z correlation.

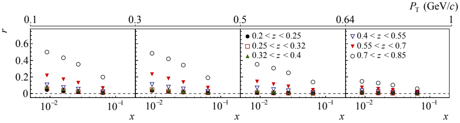

The contamination fraction: 3D(P_{T}, z, x) representation.

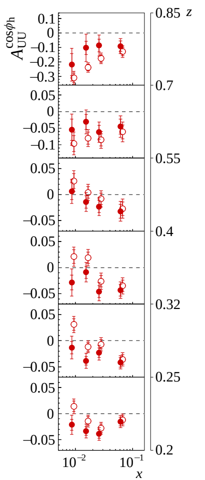

Before (empty) and after (full) subtraction.

$0.1 < P_{\mathrm{T}}/(\mathrm{GeV}/c) < 0.3$.

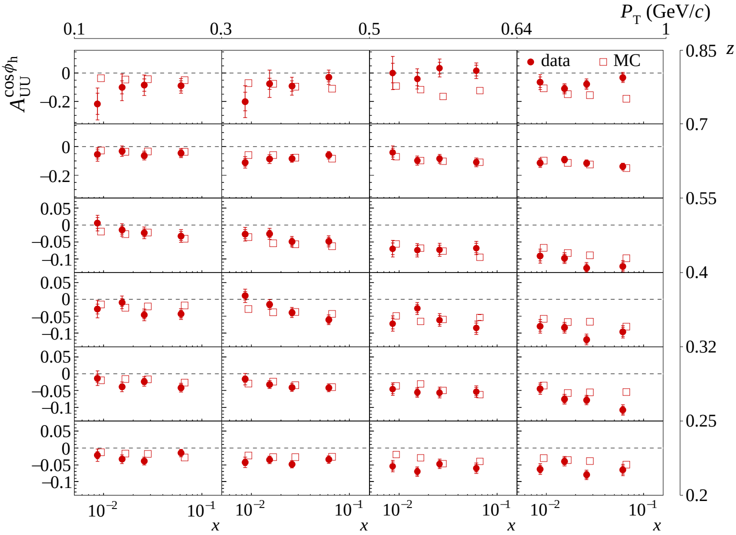

After exclusive VM decay contribution is subtracted, rather good agreement with an MC model based on Cahn effect and string fragmentation [A. Kerbizi *et al.*, Phys.Rev.D 97 (2018)] can be reached [COMPASS, Nucl.Phys.B 956 (2020)].

Outline

New measurements on LH_2: Event selection and binning

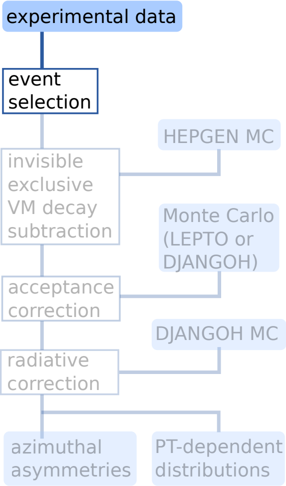

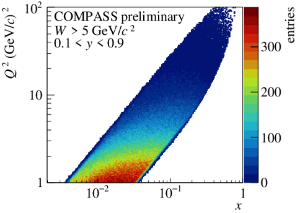

The x and Q^2 range covered.

DIS event selection

- $Q^2 > 1\ (\mathrm{GeV}/c)^2$,
- $W > 5\ \mathrm{GeV}/c^2$,
- $0.003 < x < 0.13$,
- $0.2 < y < 0.9$,
- $\theta_\gamma < 60$ mrad,
- Exclusive VM decay cut: if only $\mu' h^+ h^-$ outgoing, $z_1 + z_2 = z_t < 0.95$.

Hadron selection

- $0.1 < z < 0.85$,
- $0.1 < P_T/(\mathrm{GeV}/c) < 1.73$.

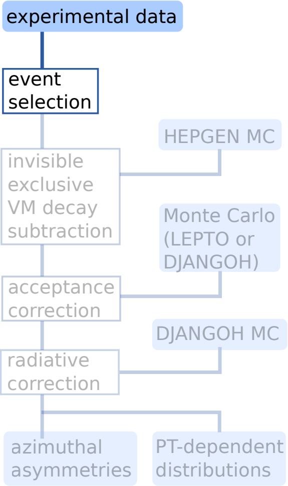

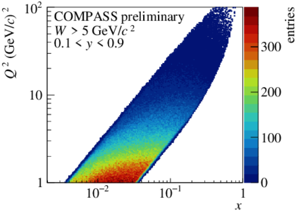

The x and Q^2 range covered.

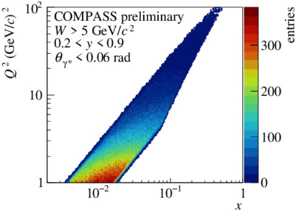

Selected range with moderate acceptance corrections.

DIS event selection

- $Q^2 > 1\ (\mathrm{GeV}/c)^2$,
- $W > 5\ \mathrm{GeV}/c^2$,
- $0.003 < x < 0.13$,
- $0.2 < y < 0.9$,
- $\theta_\gamma < 60$ mrad,
- Exclusive VM decay cut: if only $\mu' h^+ h^-$ outgoing, $z_1 + z_2 = z_t < 0.95$.

Hadron selection

- $0.1 < z < 0.85$,
- $0.1 < P_T/(\mathrm{GeV}/c) < 1.73$.

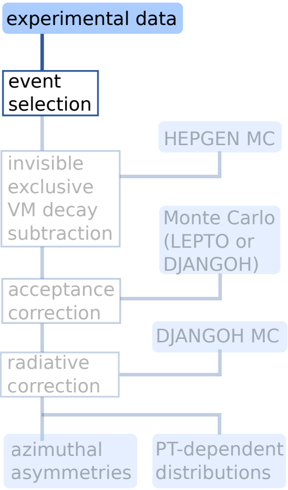

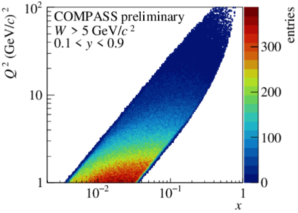

The x and Q^2 range covered.

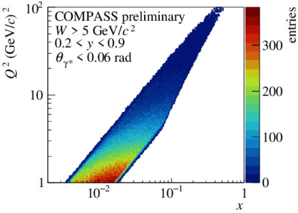

Selected range with moderate acceptance corrections.

DIS event selection

- $Q^2 > 1\ (\mathrm{GeV}/c)^2$,
- $W > 5\ \mathrm{GeV}/c^2$,
- $0.003 < x < 0.13$,
- $0.2 < y < 0.9$,
- $\theta_\gamma < 60$ mrad,
- Exclusive VM decay cut: if only $\mu' h^+ h^-$ outgoing, $z_1 + z_2 = z_t < 0.95$.

Hadron selection

- $0.1 < z < 0.85$,
- $0.1 < P_T/(\mathrm{GeV}/c) < 1.73$.

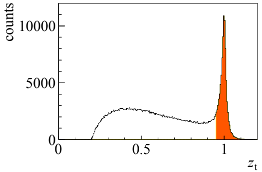

[COMPASS, Nucl.Phys.B 956 (2020)]

New measurements on LH_2: Event selection and binning

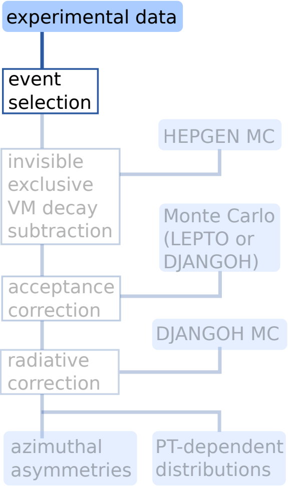

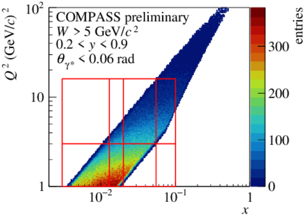

Q^2 and x bins for the P_{T}-dependent distributions.

Binning

- Based on the published results.
- Asymmetries:
  - 1D in x, z and P_{T}.
  - 3D in x, z and P_{T}
- P_{T}-dependent distributions
  - 4D in x, Q^2, z and P_{T}^2.
  - Larger bins w.r.t the publication (2 bins in every variable merged).

New measurements on LH_2: Exclusive VM decay subtraction

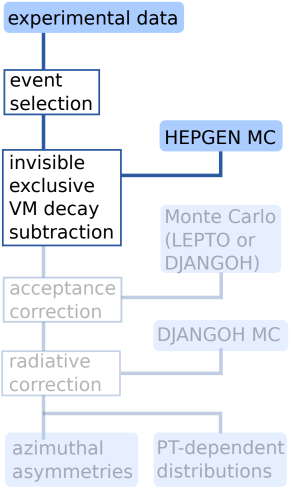

- Different approach w.r.t published d asymmetries.
- 'Visible' exclusive h^+h^- removed in event selection.
  - About 80 % of the decays are 'visible'.
- 'Invisible' decays (only one h observed)
  - HEPGEN MC generator with azimuthal modulations.
  - Normalised to the data using E_{miss} distribution of the 'visible' decays.
  - Subtracted in every bin (including ϕ_h bins).

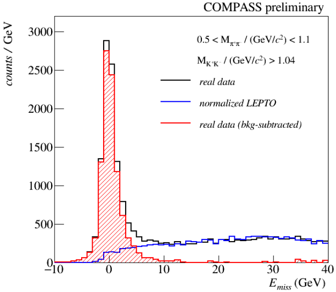

The number of signal events in the peak after SIDIS (from LEPTO) background subtraction is used to normalise HEPGEN.

New measurements on LH_2: Exclusive VM decay subtraction

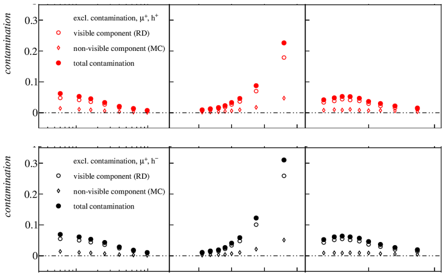

The VM-contamination fraction.

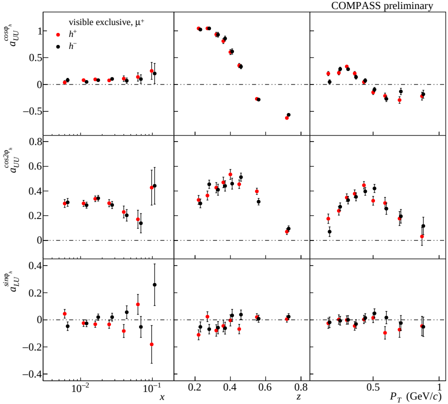

The azimuthal modulations of hadrons from the 'visible' VM decays. The 'invisible' ones have very similar modulations.

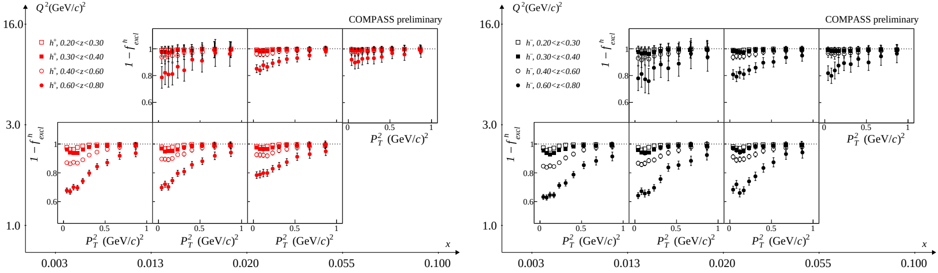

The impact of the VM-subtraction ('visible' and 'invisible') on the P_{T}-dependent distributions.

New measurements on LH_2: Results for the asymmetries

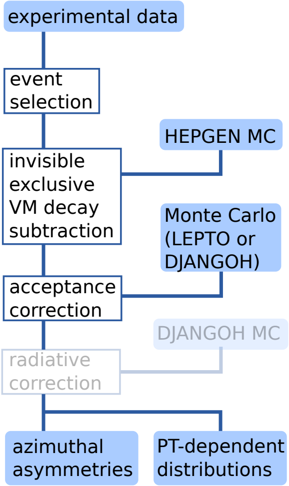

- Acceptance correction
  - LEPTO generator, full Geant simulation of COMPASS.
- QED radiative effects – not yet taken into account
  - Plan to use DJANGOH generator [DJANGO6] (→ evaluate impact on hadronic variables as well)
- 1D results
  - Strong kinematic dependences, differences between $h^{\pm}$,
  - qualitative agreement with published deuteron results [COMPASS, Nucl.Phys.B 886 (2014)].

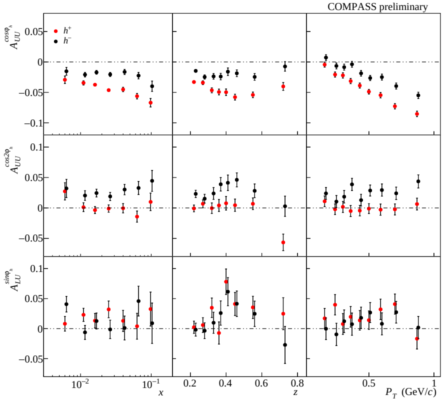

New measurements on LH_2: Results for the asymmetries

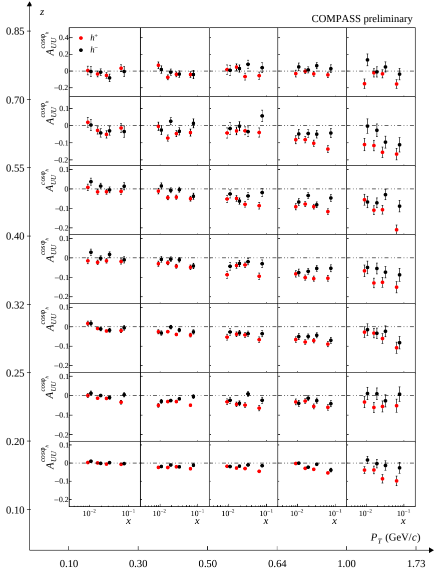

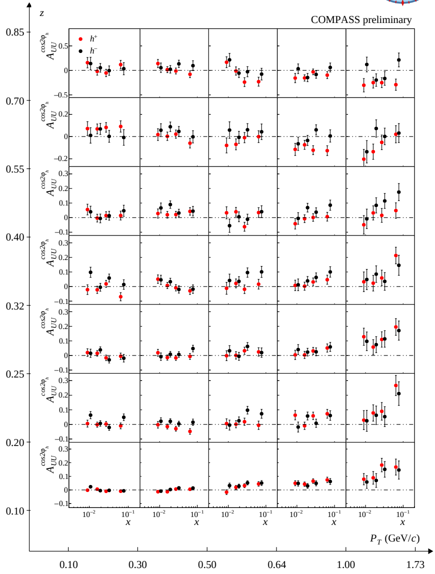

Qualitative agreement with published deuteron results [COMPASS, Nucl.Phys.B 956 (2020)].

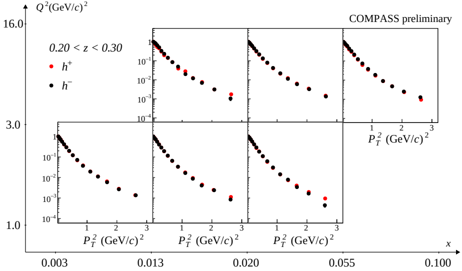

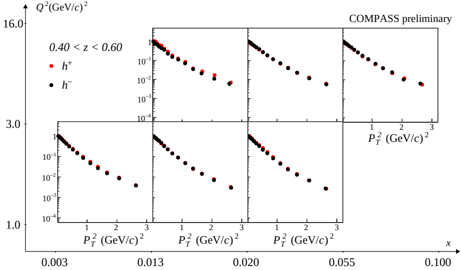

- The distributions are normalised to the first bin.
- Gaussian model for f_1 and D_1:

$$\frac{\mathrm{d}^2 N}{\mathrm{d}z\mathrm{d}P_\mathrm{T}} \propto \exp\left(-\frac{P_\mathrm{T}^2}{\langle P_\mathrm{T}^2 \rangle}\right)$$

$$\langle P_\mathrm{T}^2 \rangle = z^2 \langle k_\mathrm{T}^2 \rangle + \langle p_\perp^2 \rangle.$$

- Deviation from the simple exponential visible at $P_\mathrm{T} > 1$ (GeV/c)^2.

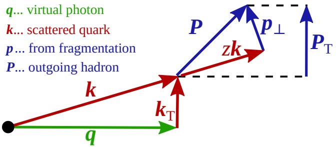

New measurements on LH_2: Results for the P_T-distributions

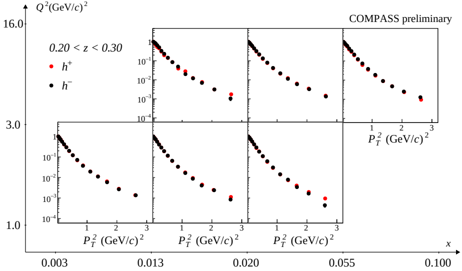

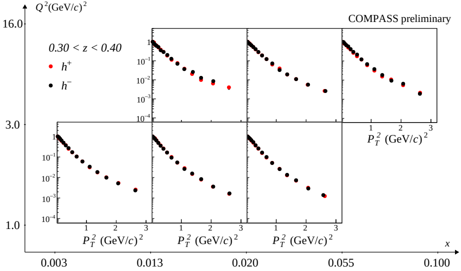

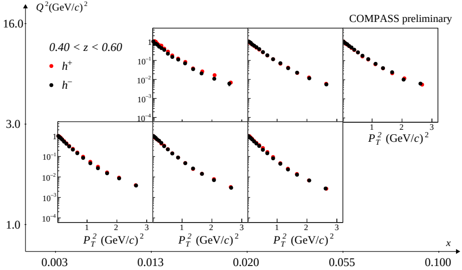

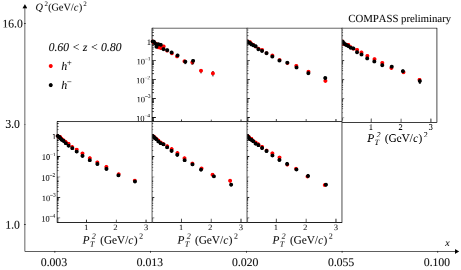

New measurements on LH_2: Results for the P_T-distributions

COMPASS

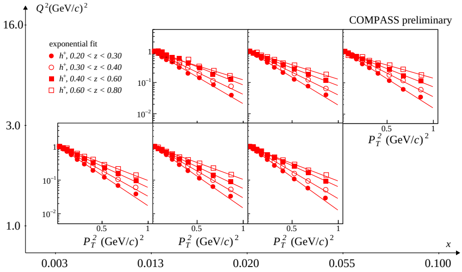

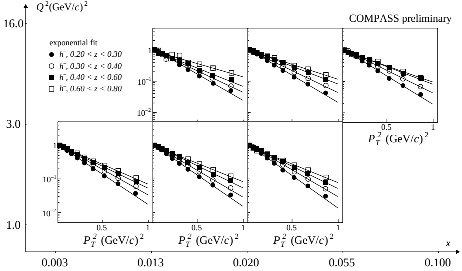

Exponential fit in $P_\mathrm{T} < 1\ (\mathrm{GeV}/c)^2$ range.

$$\frac{\mathrm{d}^2 N}{\mathrm{d}z\mathrm{d}P_\mathrm{T}} \propto \exp\left(-\frac{P_\mathrm{T}^2}{\langle P_\mathrm{T}^2\rangle}\right)$$

- Deviations from the linear trend expected from the simple Gaussian model

$$\langle P_\mathrm{T}^2\rangle = z^2\langle k_\mathrm{T}^2\rangle + \langle p_\perp^2\rangle.$$

- Possible dependence of $\langle p_\perp^2\rangle$ on z or of $\langle k_\mathrm{T}^2\rangle$ on x.

New measurements on LH_2: Results for the P_{T}-distributions

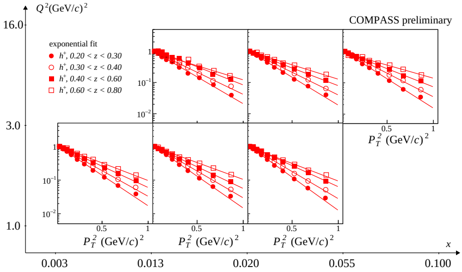

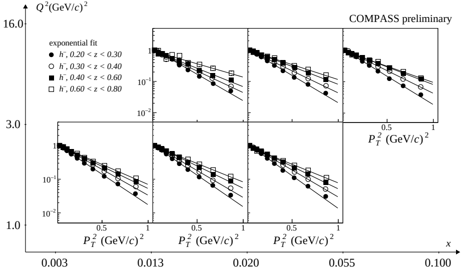

Exponential fit in $P_{\mathrm{T}} < 1\ (\mathrm{GeV}/c)^2$ range.

$$\frac{\mathrm{d}^2 N}{\mathrm{d}z\mathrm{d}P_{\mathrm{T}}} \propto \exp\left(-\frac{P_{\mathrm{T}}^2}{\langle P_{\mathrm{T}}^2\rangle}\right)$$

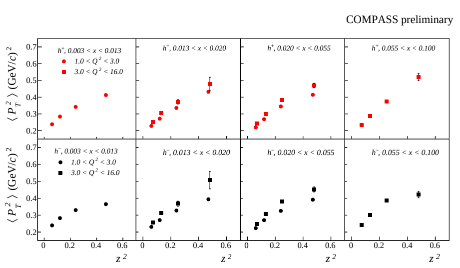

The fitted $\langle P_{\mathrm{T}}^2\rangle$ versus z^2 in the x and Q^2 bins.

- Deviations from the linear trend expected from the simple Gaussian model

$$\langle P_{\mathrm{T}}^2\rangle = z^2\langle k_{\mathrm{T}}^2\rangle + \langle p_{\perp}^2\rangle.$$

- Possible dependence of $\langle p_{\perp}^2\rangle$ on z or of $\langle k_{\mathrm{T}}^2\rangle$ on x.

Outline

Conclusion

Interesting observables in unpolarised SIDIS

- Azimuthal asymmetries: sensitive to k_T (via Cahn effect) and to Boer–Mulders function.
- P_T-dependent distributions: sensitive to k_T and $p_\perp$ dependence of f_1 and D_1.
- Contamination from decays of exclusive VMs plays an important role in both measurements.

COMPASS measurements

- Published results on ^{6}LiD target: [COMPASS, Nucl.Phys.B 886 (2014)], [COMPASS, Phys.Rev.D97 (2018)], [COMPASS, Nucl.Phys.B 956 (2020)].
- New preliminary results (August 2020) on liquid H_2 target.
  - 11 % of the statistics,
  - More robust method for exclusive VM subtraction.
  - Alternating $\mu^\pm$ beam – systematic check.
  - Qualitative agreement with deuteron, rich kinematic dependences.
  - More results will come.
- Scheduled 2021 measurement with (transversely polarised) ^{6}LiD target.

These measurements provide important input to general understanding of the transverse-momentum-dependent structure of the nucleon and of the fragmentation process.

Conclusion

Interesting observables in unpolarised SIDIS

- Azimuthal asymmetries: sensitive to k_T (via Cahn effect) and to Boer–Mulders function.
- P_T-dependent distributions: sensitive to k_T and $p_\perp$ dependence of f_1 and D_1.
- Contamination from decays of exclusive VMs plays an important role in both measurements.

COMPASS measurements

- Published results on ^{6}LiD target: [COMPASS, Nucl.Phys.B 886 (2014)], [COMPASS, Phys.Rev.D97 (2018)], [COMPASS, Nucl.Phys.B 956 (2020)].
- New preliminary results (August 2020) on liquid H_2 target.
  - 11 % of the statistics,
  - More robust method for exclusive VM subtraction.
  - Alternating $\mu^\pm$ beam – systematic check.
  - Qualitative agreement with deuteron, rich kinematic dependences.
  - More results will come.
- Scheduled 2021 measurement with (transversely polarised) ^{6}LiD target.

These measurements provide important input to general understanding of the transverse-momentum-dependent structure of the nucleon and of the fragmentation process.

Thank you for your attention!

Backup: Kinematic distributions

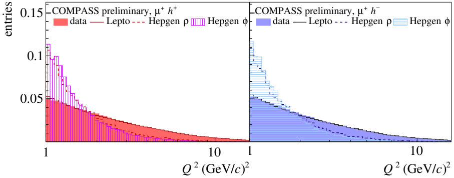

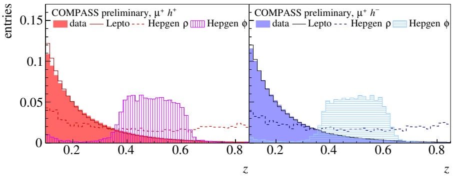

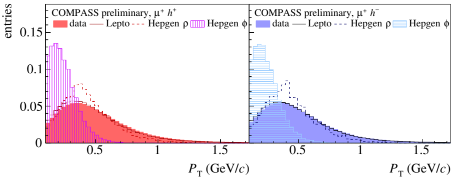

Normalised kinematic distributions: real data, LEPTO, HEPGEN ρ^0 and HEPGEN ϕ.

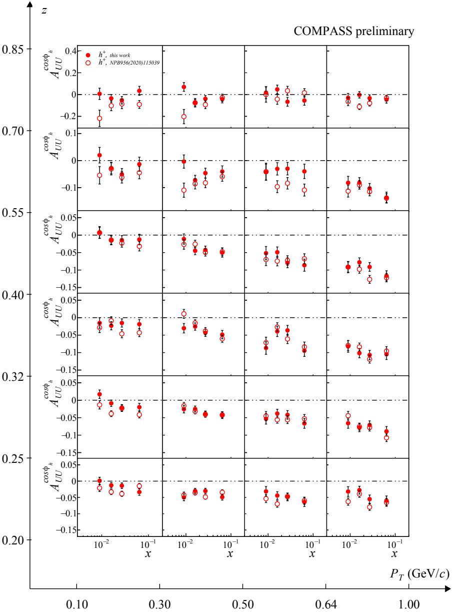

COMPASS preliminary
z
0.85
0.70
0.55
0.40
0.32
0.25
0.20
h^+, this work
h^+, NPB956(2020)115039
$A_{UU}^{\cos\phi_h}$
x
P_T (GeV/c)
0.10
0.30
0.50
0.64
1.00

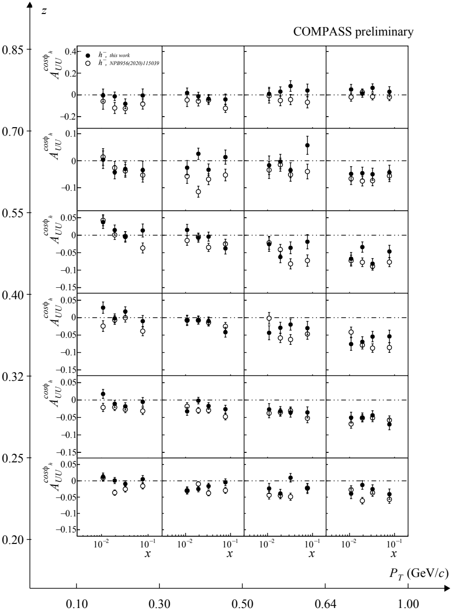

COMPASS preliminary
z
0.85
0.70
0.55
0.40
0.32
0.25
0.20
h^-, this work
h^-, NPB956(2020)115039
$A_{UU}^{\cos\phi_h}$
x
P_T (GeV/c)
0.10
0.30
0.50
0.64
1.00

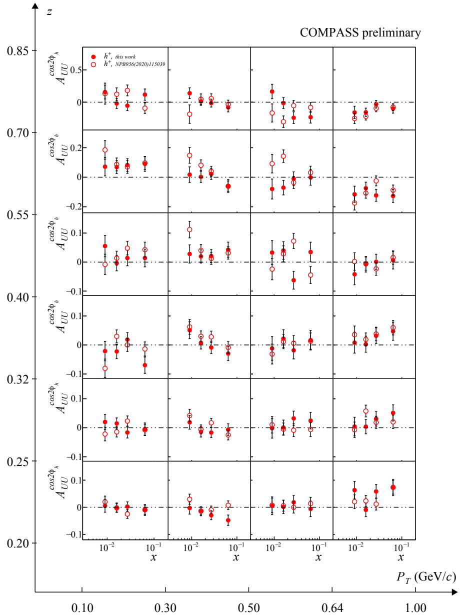
COMPASS preliminary
z
0.85
0.70
0.55
0.40
0.32
0.25
0.20
h^+, this work
h^+, NPB956(2020)115039
$A_{UU}^{\cos2\phi_h}$
x
P_T (GeV/c)
0.10
0.30
0.50
0.64
1.00

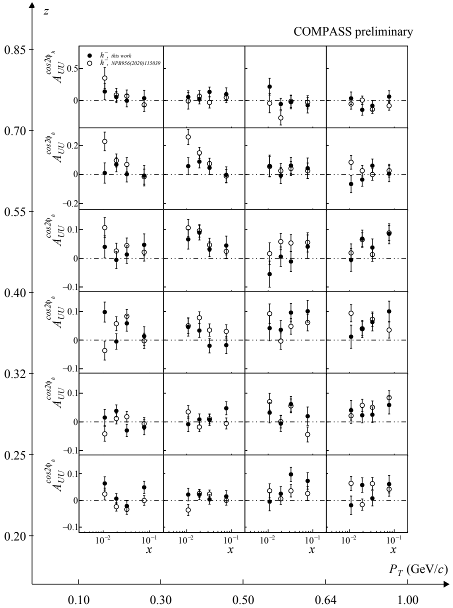
COMPASS preliminary
z
0.85
0.70
0.55
0.40
0.32
0.25
0.20
h^-, this work
h^-, NPB956(2020)115039
$A_{UU}^{\cos2\phi_h}$
x
P_T (GeV/c)
0.10
0.30
0.50
0.64
1.00

Backup: Comparison of the P_T-distributions with deuteron